Dynamics of polarization reversal in virgin and fatigued ferroelectric ceramics by inhomogeneous field mechanism

Sergey Zhukov, Yuri A. Genenko, Ofer Hirsch, Julia Glaum, Torsten Granzow, and Heinz von Seggern*
Institute of Materials Science, Technische Universität Darmstadt, Petersenstrasse 23, 64287 Darmstadt, Germany
(Received 9 March 2010; revised manuscript received 14 May 2010; published 19 July 2010)

Temporal behavior of ferroelectric ceramics during the polarization switching cannot be satisfactorily explained by simple Debye or even stretched exponential laws. These materials exhibit rather a wide spectrum of characteristic times interpreted by different authors as switching or nucleation waiting times, the physical reasons for a wide time distribution still remaining unclear. A new model of polarization switching presented here suggests that the characteristic time variance in the ferroelectrics originates from the random distribution of the local electric fields due to intrinsic randomness of the material. The presented theory allows a direct extraction of the distribution of field values from the experiment. Systematic studies of polarization switching in fatigued lead zirconate titanate demonstrate the evolution of the field distribution with increasing level of fatigue. Plausible cause of the formation of regions subject to different field strengths is the generation of defects such as microcracks, pores, or voids in the course of fatigue. Suitability of the proposed model is demonstrated by an excellent correlation between experimental and calculated data for virgin and differently fatigued samples in a broad time-field region covering the electric field values of 0.5–2.5 kV/mm and nine orders of the magnitude of poling time.

DOI: 10.1103/PhysRevB.82.014109 PACS number(s): 77.80.Fm, 77.84.Cg

I. INTRODUCTION

The process of polarization reversal is certainly one of the most important features of ferroelectric materials. A large number of models describing this process has been proposed up to now.[1–11] Most of those models are based on the so-called Kolmogorov-Avrami-Ishibashi (KAI) approach,[1–4] which considers the switching process to occur in two basic stages: (1) nucleation and (2) growth of reversed domains. Some authors divide the second stage additionally in two steps in order to separate forward and sidewise domain-wall motion. Often the sidewise motion is supposed to be the slow stage during polarization reversal.[6,7] Depending on the model, the switching process is described as being dominated either by the rate of nucleation or by the mobility of domain walls. There are also some alternatives to the KAI model which do not consider nucleation and domain-wall motion at all and describe polarization reversal by a specific relaxation mechanism[8] or introducing the Preisach distribution (Preisach model) for ferroelectrics.[9] Another alternative is the representation of the ferroelectric volume as an ensemble of elementary regions characterized by different switching times (or nucleation waiting times in terms of Ref. 10) with smooth and exponentially broad distribution of these times covering many decades. The question remaining is for the physical origin of the latter broad distribution. Taking into account the field dependence of the switching process an inhomogeneous field distribution in ferroelectric samples was discussed as a possible reason for the switching time distribution in Ref. 12 but no quantitative model was suggested.

Recently we have presented an inhomogeneous field mechanism (IFM) of polarization dynamics in ferroelectric ceramics based on two principal assumptions: (1) a strong dependence of the polarization switching time τ on the local electric field and (2) a random distribution of the local switching times due to intrinsic randomness of the field distribution in the system.[13] Comparison of the switching dynamics for different applied fields revealed the existence of a distribution of local electric field values which is characteristic for the system. Moreover, the experimental data indicated that the field distribution is virtually independent on poling time and remains constant at all poling stages. We suggested that such random-field distribution can be described by a Gaussian distribution around the applied field strength E_m. By considering the ferroelectric volume as an ensemble of many regions with independent switching dynamics, governed by a local electric field exclusively, and assuming the very simple approximation of immediate switching of polarization in the regions of the sample when the observation time exceeds the local switching time we obtained an explicit total polarization dependence ΔP on time t and applied field E_m,

$$\Delta P(E_m,t) = P_r \,\mathrm{erfc}\left[\frac{\frac{E_a}{E_m \ln(t/\tau_0)} - 1}{\sigma\sqrt{2}}\right], \qquad (1)$$

where all the parameters can be determined experimentally. P_r is the maximum remanent polarization, E_a and τ_0 characterize the field-dependent local switching time $\tau(E)$ of those regions subjected to the local field E, and σ is the variance of the Gaussian distribution function.

It was demonstrated[13] that the proposed IFM model provides a good description of polarization dynamics in unfatigued lead zirconate titanate (PZT) ceramics in a broad time-field domain. Only minor discrepancies from the experimental data were observed at the initial stage of the polarization reversal process. This discrepancy was ascribed to a partly incorrect approximation of the real field distribution in ferroelectrics by a Gauss type function.

In the present paper we intend to demonstrate an advanced approach to polarization switching which can more properly identify the real local-field distribution function and thus provide a better description of the experimental data for unfatigued PZT ceramics. Furthermore, it will be shown that the IFM approach can be successfully applied to fatigued ceramics and how the local-field distribution can be directly extracted from the polarization measurements without specific model assumptions on the time and field dependence of the local polarization. Then the evolution of the local-field distribution during fatigue will be investigated. In the first part of the paper the experimental setup and the measurement method are presented. In the second part the suggested model is described in detail and then, in the third part, it is applied to the unfatigued as well as to the fatigued PZT ferroelectric. In the concluding part of the paper physical reasons for the random distributions of the local electric fields relevant to the experiment are discussed.

II. EXPERIMENTAL

The measurements were performed on the commercial PZT polycrystalline ceramics PIC 151 ($Pb_{0.99}[Zr_{0.45}Ti_{0.47}(Ni_{0.33}Sb_{0.67})_{0.08}]O_3$) from PI Ceramics (Lederhose, Germany). The samples are disk shaped with 10 mm in diameter and 1 mm in thickness. The average grain size is about 6 μm. All samples have electrodes made of silver paste fired at 720 °C by the manufacturer. The samples were bipolar fatigued at a field of 2 kV/mm and a frequency of 50 Hz.

Poling and switching experiments were performed utilizing the same electrical circuit as described in Ref. 13. The actual high-voltage (HV) switching was performed by means of an electronic high-voltage/high-current push-pull switch from Behlke Co., Germany. The voltage across the sample was switched from initial ground to HV and back to ground. This allows one to stop the buildup of the polarization within the time constant of the electrical circuit, which is much shorter than the actual ferroelectric switching time of the PZT studied and shorter than the shortest voltage pulse (1 μs) applied in this investigation.

To study the polarization switching phenomenon in PZT, the samples were at first poled to saturation by applying a dc field of E_0=2 kV/mm (about twice the coercive field strength) for 1 h assuming that the maximum saturated polarization P_r has been reached. This process is called "conditioning" in the paper below. After such a conditioning, an oppositely directed switching field E_{sw} between 0.5 and 2.5 kV/mm was applied to the sample for a definite time duration t_p varied in the range between 1 μs and 10^3 s. During the switching process and the subsequent short circuiting the total displacement $D_{sw}(t)$ including the integrated conduction currents was recorded by means of a digital oscilloscope. After each switching experiment the sample was conditioned as described above to restore its initial saturated polarization. To determine the polarization ΔP reversed during application of the field E_{sw} for the time t_p, a subsequent forward poling was performed by applying the same field E_{sw} to a freshly conditioned sample in the same poling direction also for the time t_p. Since this sample was already polarized to saturation, the apparent displacement $D_{fp}(t)$ during forward poling contains all components of the switching experiment except for the permanently switched ferroelectric polarization ΔP. Therefore, the switched ferroelectric polarization ΔP can be calculated by subtracting the forward poling curve $D_{fp}(t)$ from the switching curve $D_{sw}(t)$ at any moment after application of the switching voltage pulse. This procedure was only used for times where the switching voltage was completely applied to the sample.

III. MODEL FOR POLARIZATION REVERSAL

First of all, we consider the switching volume as an ensemble of many regions with independent dynamics governed by the local field exclusively. The local-field values are randomly distributed in the bulk due to intrinsic inhomogeneities of the ferroelectric material. Nonuniform field distribution in virgin ceramics is supposed to be caused by discontinuities of the dielectric tensor at the grain boundaries between different grains which have generally independent crystal orientations. In fatigued ceramics, additional reasons for field redistribution may arise. Therefore different regions of the sample subjected to different local fields determine the inhomogeneous switching behavior. In the course of fatigue, the distribution of the random local fields changes which causes a change in the distribution of the characteristic switching times.

The main assumptions of the IFM model are listed below. (1) Switching of the local spontaneous polarization follows an arbitrary law which contains a local switching time τ. This law can, for example, be a stretched exponential dependence of the type[14]

$$p(t,\tau) = 2P_r\left\{1 - \exp\left[-\left(\frac{t}{\tau}\right)^{\beta}\right]\right\} \tag{2}$$

with β about 1. An important property of this law is that it looks similar to a step function on logarithmic time scale.

(2) The local characteristic time τ exhibits a strong dependence on the local-field value like the following empirical expression used by many authors[15,16] to correlate the switching time in ferroelectrics with the applied electric field E,

$$\tau(E) = \tau_0 \exp\left[\left(\frac{E_a}{E}\right)^{\alpha}\right], \tag{3}$$

where τ_0 is the characteristic switching time constant, E_a is an activation field, and the exponent α is about 1. This particular form of the field dependence is not essential; in fact, it will be established below experimentally.

(3) The total polarization of the system results from the summation of the local polarizations and can be represented as[10]

$$\Delta P(E_m,t) = \int_0^{\infty} d\tau g(\tau) p(t,\tau), \tag{4}$$

where $g(\tau)$ is the distribution function of the switching times in the system. This distribution function presents the fraction

of the volume of the ferroelectric characterized by switching time τ not presuming that this volume is connected. Assuming that the whole sample volume is switchable the function $g(\tau)$ can be related to the distribution function of the field values $Z(E,E_m)$ by using the relation $g(\tau)d\tau=Z(E,E_m)dE$ for a given dependence $\tau(E)$ and a mean applied electric field E_m. Using Eq. (4) the total polarization can then be described as the integral over the local-field values

$$\Delta P(E_m,t) = \int_0^\infty dEZ(E,E_m)p[t,\tau(E)]. \tag{5}$$

According to its statistical meaning the distribution function Z must be normalized,

$$\int_0^\infty dEZ(E,E_m) = 1, \tag{6}$$

and deliver the mean value of the field after averaging,

$$\int_0^\infty dEEZ(E,E_m) = E_m. \tag{7}$$

Equations (6) and (7) imply that the whole volume of the sample remains switchable and that the same dependence $\tau(E)$ is valid everywhere.

(4) The system is supposed to be a linear, random medium characterized by a field-independent dielectric permittivity which may spatially vary and be anisotropic. That is why one expects that the local values of the electric field, E, scale with the value of the mean field applied, E_m. Therefore, the distribution function of the random field acquires the form

$$Z(E,E_m) = \frac{1}{E_m} f\left(\frac{E}{E_m}\right), \tag{8}$$

which implies, according to Eqs. (6) and (7), that

$$\int_0^\infty dxf(x) = 1 \quad \text{and} \quad \int_0^\infty dxxf(x) = 1. \tag{9}$$

To obtain the function $f(x)$ from the experiment, some further simplifications are introduced. Considering Eqs. (2) and (3) we note that for all prevalent values of parameters α, β, E_a, and τ_0, the function $p[t,\tau(E)]$ can be roughly approximated[10] by the Heaviside step function with time $2P_r\cdot\theta[t-\tau(E)]$ or, with field, by $2P_r\cdot\theta[E-E_{th}(t)]$ where the characteristic time τ is defined by the inflection point of the function $p[t,\tau(E)]$ on the logarithmic time scale and the threshold field $E_{th}(t)$ results from the solution of equation $t=\tau(E)$. The physical meaning of this approximation is that the polarization reversal occurs immediately in regions where the local characteristic time $\tau(E)$ is exceeded by the elapsed time t of voltage application or, in terms of the field, when the local electric field E exceeds the time-dependent threshold field $E_{th}(t)$. Then the polarization $\Delta P(E_m,t)$ in Eq. (5) simply results from integration of the distribution $Z(E,E_m)$ from $E_{th}(t)$ to infinity,

$$\Delta P(E_m,t) \cong 2P_r \int_{E_{th}(t)}^\infty dEZ(E,E_m). \tag{10}$$

This presentation allows a direct extraction of the function $Z(E,E_m)$ as well as of the field dependence of the characteristic switching time from the experiment. Most conveniently it can be done considering the derivative of the polarization with respect to the applied field for different values of the time which exhibits a time-dependent maximum. Specifically, the logarithmic derivative of the polarization [Eq. (10)] reads

$$\frac{E_m}{2P_r}\frac{\partial\Delta P(E_m,t)}{\partial E_m} = \frac{1}{\eta}f\left(\frac{1}{\eta}\right), \tag{11}$$

where $\eta=E_m/E_{th}(t)$. Form (11) implies that experimental dependencies of the logarithmic derivative on the applied field taken for different times should be reducible to the same curve $\Phi[E_m/E_{\max}(t)]$, where $E_{\max}(t)$ is the position of the maximum of this derivative at time t. When this scaling property is actually observed in the experiment, the validity of the model assumptions 1–4 is confirmed. From its definition, the master curve $\Phi(x)$ has a maximum at $x=1$ and its exact form contains information on the statistical distribution of the local-field values. Comparing the left- and right-hand sides of Eq. (11) it is clear that the threshold field $E_{th}(t)$ must be proportional to $E_{\max}(t)$, namely, $E_{\max}(t)=\gamma E_{th}(t)$, where γ is a constant. Then, using Eq. (11), the distribution function can be obtained from the identity

$$f(x) = \frac{1}{x}\Phi\left(\frac{1}{\gamma x}\right). \tag{12}$$

The constant γ should be determined from the normalization conditions, Eq. (9). The first of these equations is satisfied for any $\gamma>0$ if the full change in the polarization from zero field to high-field values amounts to $2P_r$. From the second equation of Eq. (9) one obtains, after substituting of Eq. (12), the following relation for γ:

$$\gamma = \int_0^\infty \frac{dx}{x^2}\Phi(x), \tag{13}$$

which allows for the determination of γ from the known form of the master curve.

Another case should be discussed, namely, what happens if in the course of fatigue some part of the material becomes nonswitchable, for instance, by blocking or pinning the switching regions. This means that, in the blocked regions, the characteristic time τ becomes effectively infinite and the relation $g(\tau)d\tau=Z(E,E_m)dE$ is no more valid. Then the integration in Eqs. (4) and (5) should be understood to cover the switchable regions only. Assuming that these regions are still subject to the same mean external field the normalization conditions (6), (7), and (9) remain valid but the factor $2P_r$ in Eqs. (10) and (11) should be substituted by the mean value of the polarization in the sample which is, in fact, $2P_r$ times the fraction of the volume taken by the switchable part of the sample.

As it is clear from Eq. (10), the two functions $Z(E,E_m)$ and $E_{th}(t)$ should be determined in order to calculate the switched polarization. The first function reflects the field distribution within the ferroelectric volume at the initial stage, i.e., when the external field is switched on while the second

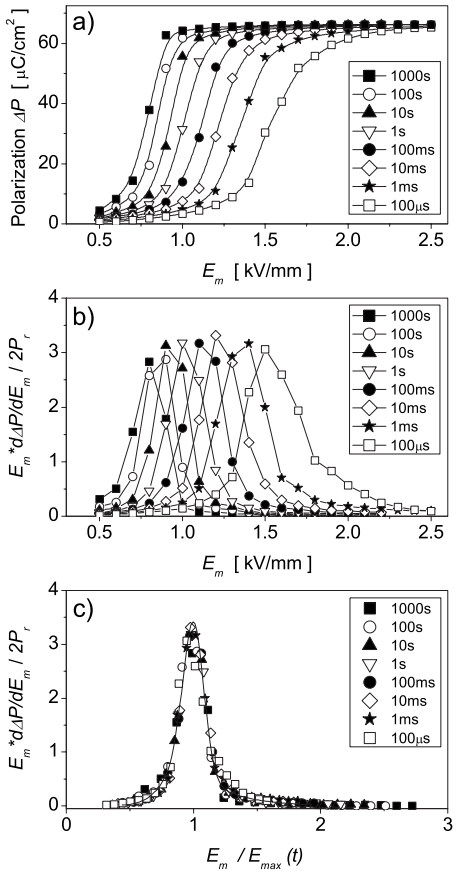

FIG. 1. (a) Switched polarization ΔP, (b) its logarithmic derivative versus applied field, and (c) logarithmic derivative versus scaled field $E/E_{\max}(t)$ for unfatigued PIC 151 ceramic at different poling time t_p as indicated.

one describes the temporal behavior of the local threshold field. Both characteristics have a crucial impact on the polarization dynamics. Therefore it is necessary to derive them with maximum accuracy. We show in the following how both functions can be extracted from charge measurements on polarization reversals.

IV. EXPERIMENTAL DETERMINATION OF THE DISTRIBUTION FUNCTION $Z(E,E_m)$ and $E_{th}(t)$

At first step, the switched polarization ΔP as function of time for different applied fields E_m has been measured and subsequently presented as function of the applied field E_m for different durations of the poling pulse t_p. Figure 1(a) displays the typical experimental dependencies obtained on the unfatigued ferroelectric ceramic PIC 151 for poling pulses ranging from 100 μs to 10^3 s. As one can see from Fig. 1(a), the complete switching of polarization strongly depends on the poling time t_p and the applied field E_m. For example, at a high field of 2.0 kV/mm, the full switching already occurs during a short voltage pulse of 100 μs whereas at 0.9 kV/mm the switching is not completed until a pulse length of 10^3 s. In the fully switched regime, ΔP reaches a polarization of 66.3 μC/cm^2 which corresponds to $2P_r$. Figure 1(b) displays the product of E_m and the derivative $d\Delta P/dE_m$ divided by $2P_r$ plotted versus the applied field E_m for the different pulse durations as indicated. Important is that each curve in Fig. 1(b) displays a maximum, whose amplitude is virtually independent on the poling pulse duration and exhibits a similar shape with a characteristic width, which increases for decreasing t_p. Since the data points are scattered the data sets for certain poling times t_p were first spline fitted and then the maximum position was determined from the maximum of the fitted curve. The properties of the logarithmic derivatives presented in Fig. 1(b) allow us to reduce all the measured dependencies to one general form by simple scaling of the applied field as can be seen from Fig. 1(c). It is seen that all the scaled data points fall on a master curve $\Phi(x)$, which will be used to restore the distribution function for local fields $f(E/E_m)$ utilizing Eq. (12). The obtained distribution is shown in Fig. 2 by solid cycles together with a hypothetic Gaussian distribution (solid line) used as ansatz function in one of our previous works for the same ceramic.[13] Note that the Gaussian constructed as suggested in Ref. 13 is centered at $x=1$ while the function $f(x)$ recovered from Eq. (12) is not. The comparison between the two functions reveals also that the left and right wings for the Gaussian distribution decay faster than those of the $f(E/E_m)$ function directly derived from the experiment. It can therefore be concluded that the Gauss function can well describe the main switching behavior but some discrepancies have to be expected at the initial (high local field) and final (low local field) poling stages. Indeed, such deviations from the experimental data were observed previously.[13]

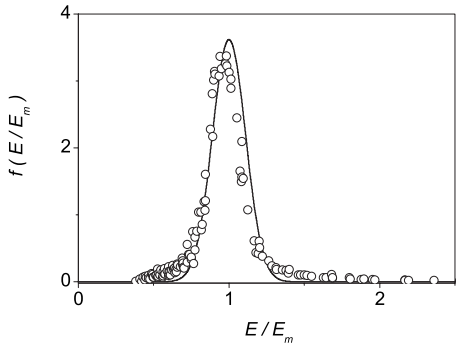

FIG. 2. Local-field distribution for virgin PIC 151 ceramic: a comparison between the $f(E/E_m)$ function derived from the experiment and the Gauss distribution with $\sigma=0.11$.

Prior to applying Eq. (10) to the calculation of the polarization reversal the temporal dependence of the threshold field $E_{th}(t)$ has to be found. Figure 3 displays the position of the maximum of the derivative in Fig. 1(b) (symbols) for various pulse durations together with the fit result (solid line) by the function $E^*/\ln(t/\tau_0)$ using $\tau_0=3.5\times10^{-12}$ s and $E^*=26.8$ kV/mm. As can be seen, the selected function provides a good fit for a whole time interval ranging over seven decades. The constant γ can be determined using Eq. (13) by numerical integration of the master curve in Fig. 2. Then the activation field $E_a=E^*/\gamma$ can be obtained resulting in the time evolution of the threshold field $E_{th}(t)=E_a/\ln(t/\tau_0)$. In the framework of the proposed model this function defines the corresponding variation in the local switching time with the field $\tau(E)=\tau_0\exp(E_a/E)$. This result is in accord with the

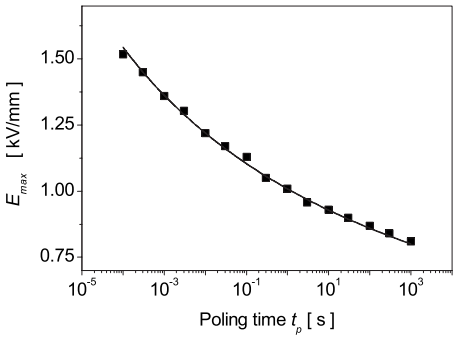

FIG. 3. Scaling field $E_{\max}(t)$ versus poling time t_p. Symbols correspond to the experimental data, whereas the solid line represents the fit by the function $E^*/\ln(t/\tau_0)$ with $E^*=26.8\pm0.6$ kV/mm and $\tau_0=(3.5\pm0.5)\times10^{-12}$ s.

utilized empirical law expressed by Eq. (3) assuming $\alpha=1$.

The above described analysis was applied to the experimental data of the polarization reversals for differently fatigued PIC 151 ceramics. In all cases we were able to extract from the experiments the local-field distributions shown in Fig. 4. One recognizes that the obtained distributions change continuously with the number of ac load cycles N, whereas for higher cycle numbers rather asymmetrical distributions with long tails on the low-field side can be observed. While such physical parameters as the maximum switchable polarization $2P_r$ and γ, listed in Table I, display gradual variation with the cycle number N, the parameters E_a and τ_0 remain virtually independent on fatigue.

V. DISCUSSION

Using the above obtained parameters the reversed polarization as a function of time can be calculated utilizing Eq. (10). The theoretical curves are shown in Fig. 5 as solid lines together with the experimental data presented by symbols for different fields applied and for different stages of fatigue indicated by the number of cycles N.

It can be seen from Fig. 5 that the model well describes the switching behavior for the unfatigued ceramic as well as for fatigued ones in a broad time window ranging over nine orders of the magnitude (from 10^{-6} to 10^{3} s) for different applied electrical fields. The samples demonstrate polarization reversal with a maximum value gradually decreasing with increasing number of cycles in comparison to $2P_r$ for the virgin sample. Thereby, the time dependencies of the polarization reversals remain qualitatively of the same shape. In accord with this observation, the respective distributions of the local fields reveal a gradual change in the height and the width maintaining at the beginning the same symmetry as the distribution for the virgin material. With increasing number of cycles the samples exhibit remarkably reduced maximum values of the reversed polarization and quasilogarithmic time behavior at large times. Accordingly, the distributions of the local fields become increasingly asymmetrical in favor of low-field values which mean according to Eq. (3) prolonged characteristic times τ.

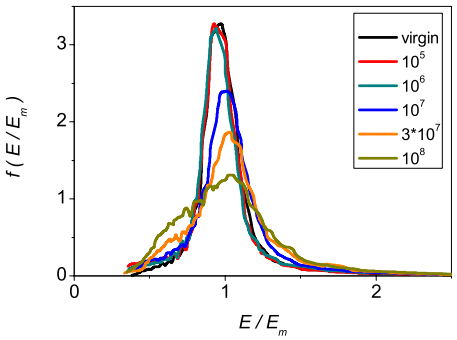

FIG. 4. (Color online) Distributions of local-field values $f(E/E_m)$ for virgin and fatigued PIC 151 ceramic as indicated.

TABLE I. The IFM-model parameters for the virgin and differently fatigued ceramics deduced from the polarization switching curves as described in Sec. IV.

Cycle number N	$2P_r$ μC/cm^2	E_a kV/mm	τ_0 s	γ
Virgin	66.4 ± 1.3	25.7 ± 0.6	$(3.5\pm0.5)\times10^{-12}$	1.043
10^5	61.9 ± 1.3	25.7 ± 0.7	$(5.9\pm0.7)\times10^{-12}$	1.043
10^6	57.5 ± 1.2	25.7 ± 0.6	$(4.7\pm0.5)\times10^{-12}$	1.054
10^7	56.0 ± 1.1	27.9 ± 0.6	$(4.4\pm0.5)\times10^{-12}$	0.987
3×10^7	52.1 ± 1.0	28.1 ± 0.7	$(5.7\pm0.6)\times10^{-12}$	0.958
10^8	48.4 ± 1.0	27.7 ± 0.6	$(1.1\pm0.2)\times10^{-11}$	0.940

There are several possible explanations for the decrease in switchable polarization due to fatigue. One mechanism that is frequently discussed is related to charged defects. These defects can either be present intrinsically in the material in the form of ions, vacancies, electrons, or holes or they can be introduced during cycling, e.g., in the form of electrons injected through the electrodes. When ionic charge carriers are considered, oxygen vacancies are usually mentioned due to their comparably high mobility.[17] Charged defects can accumulate or agglomerate where the bound charges of domains are not fully compensated,[18–20] stabilized either by domain boundaries,[18,19,21] grain boundaries,[20] the crystallographic structure,[22] or ceramic-electrode interfaces.[23] Domain walls and charged defects form a mutually stabilizing pattern, hindering further domain-wall movement and suppressing domain switching.[24]

Just like electric defects, mechanical defects and cracks can occur both in the sample volume and at the ceramic-electrode interface. Microcracking can occur as early as the first poling of a given bulk ceramic.[25] Non-180° domain switching necessarily leads to mechanical stresses within single grains and between neighboring grains, and microcracks can appear. They can be evidenced, e.g., by microscopic investigations or acoustic emission measurements.[26–28] Cracks are regions with a strongly reduced dielectric constant which cause spatial redistribution of the electric field. Kelvin probe measurements have allowed an estimation of the dielectric constant of $\varepsilon_r\approx40$ in the crack.[29] Crack formation is suppressed if the sample is subjected to compressive mechanical stress during cycling. This correlates with the observation that ferroelectrics show

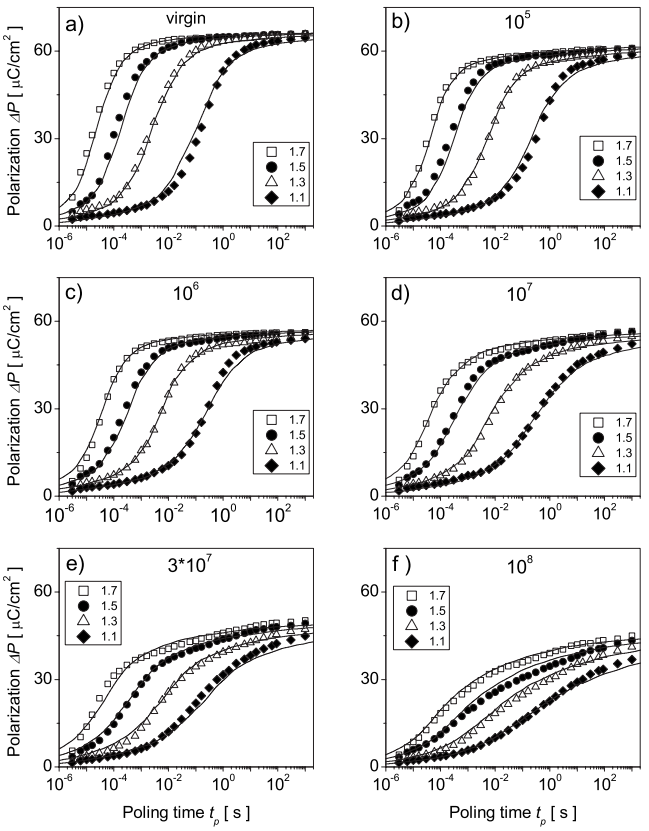

FIG. 5. (a) Switched polarization ΔP versus poling time for virgin PIC 151 ceramic and after (b) 10^5, (c) 10^6, (d) 10^7, (e) 3×10^7, and (f) 10^8 switching cycles. Symbols correspond to the experimental results measured at different fields E_m (kV/mm) as indicated. Solid curves represent the field-related model fits.

less fatigue under compressive stress conditions.[30,31]

A third possibility to explain the fatigue effects is the development of a passive dielectric layer with a low dielectric constant underneath the electrodes.[32] This "dead layer" separates the bound charges of the polarization and the compensating charges of the electrodes, leading to the appearance of a depolarizing field. The bulk of the sample is effectively shielded from the externally applied field, reducing domain switching. As the ceramic-electrode interface is a region of increased defect density, it is also the main site to nucleation of new domains. If the interface changes due to the formation of a dead layer or the accumulation of defects, the nucleation process can also be altered. If local nucleation centers are removed, the regions involved become ferroelectrically inactive, reducing the amount of switchable polarization.

Judging from the development of the local-field distribution with fatigue cycle number (Fig. 4), it seems plausible that two different mechanisms are at work in our material: the first one leads to a simple reduction in the switchable polarization without notable changes to the dynamics. It is dominant up to 10^7 fatigue cycles. The second mechanism causes the appearance of the low-field tail of the local-field distribution at cycle number of 3×10^7 and above and the corresponding long-time dynamics in the $\Delta P(t)$ curves. Neither of these mechanisms is related to surface damage: when the fatigue state was checked after gradually removing the surface layer by grinding and re-electroding the sample, no change was found in the fatigue state. This is unlike the results presented in Ref. 32; it shows that the formation of the surface layer strongly depends on the quality of the sample, its composition, and its electrodes.

Pinning of domain walls at charged defects is the only mechanism of those presented above that could cause a decrease in the switchable polarization at low cycle numbers. All other mechanisms would cause a change in the local distribution of the electric field, which is not observed in the experiment. It has to be noted that the pinning would have to be quite strong: it is not possible to free the pinned domain walls from the pinning centers by applying a rather strong external electrical field up to 2.0 kV/mm for 10^3 s [see Figs. 5(b)–5(f)].

The question remains as to what is happening on the microscopic or mesoscopic scale during long-term cycling. In this context, it is advisable to take a look at the fracture surface of samples in different states of fatigue. In previous work we reported on scanning electron microscope images taken for differently fatigued PIC 151 ceramics.[33] Almost no cracks were found for samples fatigued up to 10^6, i.e., in a state where no changes in the local-field distribution is observed. For cycle numbers $N\geq10^7$ the microcracks formation starts to become notable. No indications of the dead layer underneath the electrodes were detected for all samples investigated.

The formation of mesoscopic cracks which have a special symmetry can result in an asymmetric distribution of the local electric fields. To investigate theoretically the possible crack induced field distortion in the ferroelectric volume, we have modeled the two-dimensional field distributions around inclusions of the same area but of three different shapes: a round one and two elliptical ones, with the long axis oriented parallel to and normal to the external field direction, respectively (see Fig. 6). All inclusions are supposed to be characterized by a relative dielectric permittivity $\varepsilon=1$ in contrast to the surrounding medium of $\varepsilon=600$. As is seen in Fig. 6(a), the areas of the enhanced and reduced field values around the circular inclusion are equally large. However, in the case of the field applied along the longer axis of the elliptical inclusion [Fig. 6(b)] the area subject to the enhanced field values prevails over that with the reduced field values. In contrast to this, for the field applied along the shorter axis of the elliptical inclusion [Fig. 6(c)], the area subject to the reduced field values prevails substantially over that of the enhanced field. The resulting local-field distributions in the systems with inclusions of the three mentioned types are shown in Fig. 7. It can be seen from this plot that extended inclusions transversal to the field direction are in favor of the asymmetrical distributions of the local-field values similar to those extracted from the experiment on the fatigued samples as depicted in Fig. 4. This is in accordance with the obvious limiting case of the quasi-one-dimensional defect like the damaged layer at the electrode which depresses the field in the whole volume of the ferroelectric.[32]

Let us now consider the impact of thermal annealing on polarization switching dynamics which is known to have a strong effect on fatigued ceramics.[34] For that purpose the

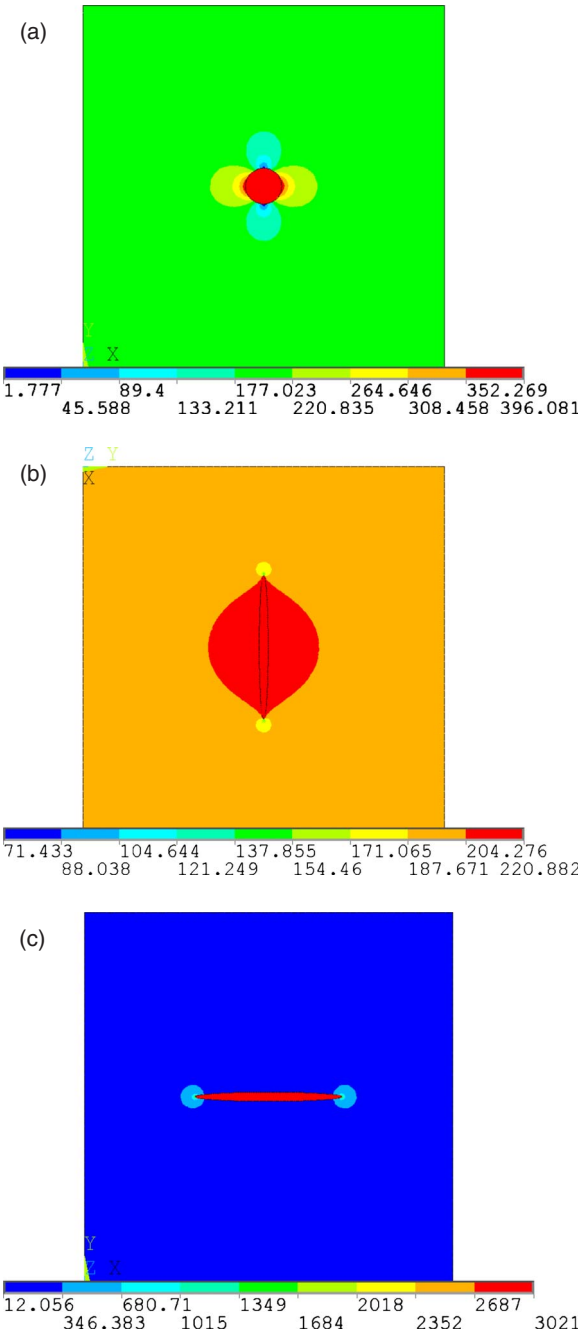

FIG. 6. (Color online) Stepwise diagram of the electric field values around the dielectric inclusions with the relative permittivity $\varepsilon=1$ inside the medium with $\varepsilon=600$. The applied field direction in figures (a)–(c) is vertical. Aspect ratio of the ellipses in figures (b) and (c) is 16:1.

fatigued samples were annealed for 24 h in air at 400 °C which is well above the Curie temperature of $T_C=250$ °C for the investigated ceramic. Figure 8 compares polarization switching of a virgin sample with a fatigued ceramic before and after annealing curves utilizing an applied field of 1.7 kV/mm. We find that for cycle numbers $\leq 10^6$ an almost complete recovery of the temporal polarization behavior after thermal annealing was obtained [see Fig. 8(a)]. For cycling times of 10^7 and larger an almost complete recovery of

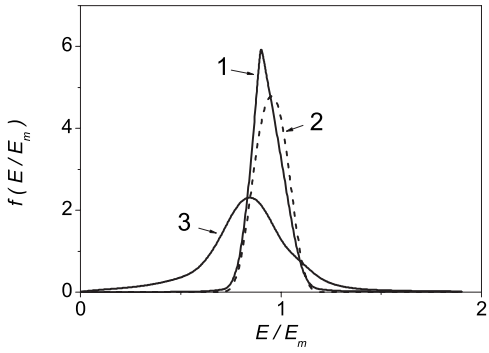

FIG. 7. Field value distributions around the inclusions shown in Fig. 6. The plot 1 corresponds to Fig. 6(a), the plot 2 to Fig. 6(b), and the plot 3 to Fig. 6(c).

the total polarization was also possible but the poling times had to be prolonged up to 10^3 s as exemplary depicted in Fig. 8(b) for a ceramic fatigued with $N=10^8$ cycles. These samples still displayed a slow quasilogarithmic component of polarization reversal as was observed before annealing. The explanation is that the thermal annealing cannot close the microcracks which then result in a broad field distribution inside the ferroelectric as was discussed above. At the same time, the loss in the switchable polarization observed at

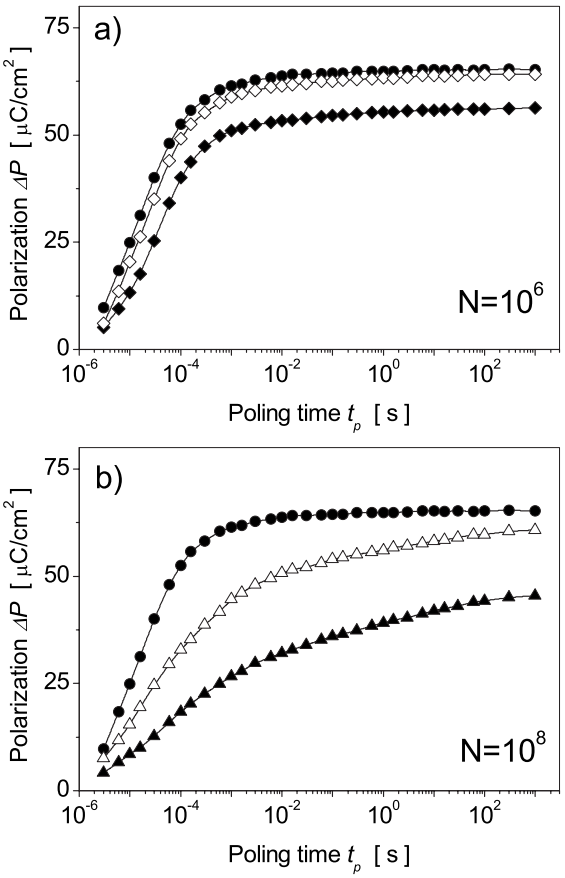

FIG. 8. Switched polarization ΔP versus poling time at an applied field $E_m=1.7$ kV/mm for the virgin (●), and fatigued at (a) $N=10^6$ and (b) $N=10^8$ cycles PIC 151 ceramics before (solid symbols) and after (open symbols) annealing at 400 °C for 24 h.

the initial stages of fatigue can be explained by charged defects acting as domain walls pinning centers which can be completely removed or redistributed by the heat treatment at temperatures above T_C. The presented results suggest that the microcracks itself cannot drastically suppress the switched polarization but can modify the local-field distribution thus causing the changes in the reversal process, i.e., considerably delay the complete switching.

VI. CONCLUSIONS

In conclusion, it was possible to describe the polarization reversal dynamics in polycrystalline PZT ceramic in virgin and fatigued state by assuming an inhomogeneous spatial distribution of the applied electric field (IFM model). During fatigue, two mechanisms were observed. The first one, dominant at low cycle numbers, causes a reduction in the switchable polarization without qualitative changes to the distribution of local-field values. Pinning of domain walls is the mechanism most likely responsible for this behavior. At higher cycle numbers, a second mechanism comes into play that changes the spatial distribution of the local electric field thus causing changes in the temporal behavior of polarization switching in favor of slow, quasilogarithmic dependences. The onset of this mechanism coincides with the appearance of cracks in the sample and impermeable cracks can account for field distributions like the ones observed. Therefore, microcracking seems the most plausible cause for the second fatigue mechanism; however, it has to be assumed that the first mechanism continues to be effective in the high cycle number regime as well.

ACKNOWLEDGMENT

The authors acknowledge the financial support by Deutsche Forschungsgemeinschaft (DFG) through Grant No. Sonderforschungsbereich (SFB) 595.

*Author to whom correspondence should be addressed; seggern@e-mat.tu-darmstadt.de

[1] E. Fatuzzo and W. J. Merz, Phys. Rev. **116**, 61 (1959).
[2] A. N. Kolmogorov, Izv. Akad. Nauk SSSR, Ser. Math. **1**, 355 (1937) [Bull. Acad. Sci. USSR, Ser. Math. **1**, 355 (1937)].
[3] M. Avrami, J. Chem. Phys. **8**, 212 (1940).
[4] Y. Ishibashi, Ferroelectrics **98**, 193 (1989).
[5] H. Orihara, S. Hashimoto, and Y. Ishibashi, J. Phys. Soc. Jpn. **63**, 1031 (1994).
[6] W. J. Merz, Phys. Rev. **95**, 690 (1954).
[7] V. Shur, E. Rumyantsev, and S. Makarov, J. Appl. Phys. **84**, 445 (1998).
[8] O. Lohse, M. Grossmann, U. Boettger, D. Bolten, and R. Waser, J. Appl. Phys. **89**, 2332 (2001).
[9] A. T. Bartic, D. J. Wouters, H. E. Maes, J. T. Rickes, and R. M. Waser, J. Appl. Phys. **89**, 3420 (2001).
[10] A. K. Tagantsev, I. Stolichnov, N. Setter, J. S. Cross, and M. Tsukada, Phys. Rev. B **66**, 214109 (2002).
[11] H. M. Duiker and P. D. Beale, Phys. Rev. B **41**, 490 (1990).
[12] D. C. Lupascu, S. Fedosov, C. Verdier, J. Rödel, and H. von Seggern, J. Appl. Phys. **95**, 1386 (2004).
[13] S. Zhukov, Y. A. Genenko, and H. von Seggern J. Appl. Phys. **108**, 014106 (2010).
[14] A. K. Jonscher, *Universal Relaxation Law* (Chelsea Dielectrics Press, London, 1996).
[15] W. J. Merz, J. Appl. Phys. **27**, 938 (1956).
[16] H. H. Wieder, J. Appl. Phys. **31**, 180 (1960).
[17] I. K. Yoo and S. B. Desu, Phys. Status Solidi A **133**, 565 (1992).
[18] Y. A. Genenko and D. C. Lupascu, Phys. Rev. B **75**, 184107 (2007); **76**, 149907(E) (2007).
[19] Y. A. Genenko, Phys. Rev. B **78**, 214103 (2008).
[20] Y. A. Genenko, J. Glaum, O. Hirsch, H. Kungl, M. J. Hoffmann, and T. Granzow, Phys. Rev. B **80**, 224109 (2009).
[21] C. Brennan, Ferroelectrics **150**, 199 (1993).
[22] J. F. Scott and M. Dawber, Appl. Phys. Lett. **76**, 3801 (2000).
[23] M. Dawber and J. F. Scott, Appl. Phys. Lett. **76**, 1060 (2000).
[24] T. Granzow, U. Dörfler, Th. Woike, M. Wöhlecke, R. Pankrath, M. Imlau, and W. Kleemann, Phys. Rev. B **63**, 174101 (2001).
[25] E. C. Subbarao, V. Srikanth, W. Cao, and L. E. Cross, Ferroelectrics **145**, 271 (1993).
[26] H.-T. Chung, B.-C. Shin, and H.-G. Kim, J. Am. Ceram. Soc. **72**, 327 (1989).
[27] Q. Jiang, E. C. Subbarao, and L. E. Cross, Acta Metall. Mater. **42**, 3687 (1994).
[28] D. C. Lupascu and M. Hammer, Phys. Status Solidi A **191**, 643 (2002).
[29] G. A. Schneider, F. Felten, and R. M. McMeeking, Acta Mater. **51**, 2235 (2003).
[30] T. Kumazawa, Y. Kumagai, H. Miura, M. Kitano, and K. Kushida, Appl. Phys. Lett. **72**, 608 (1998).
[31] Y. Fotinich and G. P. Carman, J. Appl. Phys. **88**, 6715 (2000).
[32] N. Balke, H. Kungl, T. Granzow, D. C. Lupascu, M. J. Hoffmann, and J. Rodel, J. Am. Ceram. Soc. **90**, 3869 (2007).
[33] S. Zhukov, S. Fedosov, J. Glaum, T. Granzow, Y. A. Genenko, and H. von Seggern J. Appl. Phys. **108**, 014105 (2010).
[34] C. Verdier, D. C. Lupascu, H. von Seggern, and J. Rödel, Appl. Phys. Lett. **85**, 3211 (2004).